SYNTHESIS REPORT

FOR PUBLICATION

CONTRACT N° : BREU.0182.C

PROJECT N° : BE-3038-89

TITLE : **Damage Tolerance and Fatigue Design Methodology for Primary Composite Structures**

PROJECT COORDINATOR : **E. Redondo, CASA, Getafe-Madrid (E)**

PARTNERS :

- BASF AG, D-67063 Ludwigshafen
  (Subcontractor: Institut fur Werkstoffkunde und -prüfung der Kunststoffe, Montanuniversität Leoben A-8700 Leoben)
- CASA, E-200906 Getafe-Madrid
- Fraunhofer-Institut für Betriebsfestigkeit (FhG-LBF), D-64289 Darmstadt

STARTING DATE : **August** 1,1990 DURATION : **5 6** MONTHS

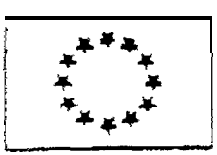

PROJECT FUNDED BY THE EUROPEAN COMMUNITY UNDER THE BRITE/EURAM PROGRAMME

DATE : **March 20, 1995**

DAMAGE TOLERANCE AND FATIGUE DESIGN METHODOLOGY FOR PRIMARY COMPOSITE STRUCTURES

R.W. Lang[1], J.J. Gerharz[2], A. Lavia[3] and M. Heym[4]

1) Institut für Werkstoffkunde und -prüfung der Kunststoffe, Montanuniversität Leoben, A-8700 Leoben
2) Fraunhofer-Institut für Betriebsfestigkeit, D-64289 Darmstadt
3) C.A.S.A., E-200906 Getafe-Madrid
4) Kunststofflaboratorium, BASF AG, D-67063 Ludwigshafen

The main purpose of this 4.5-year research program was to develop and describe a procedure that allows for an analytical prediction or at least an empirical assessment of the damage tolerance and fatigue behavior of composite subcomponents or fill scale components based on properties of smaller size specimens of the test pyramid. The new analytical design tool includes laminate plate theory, stability theory, composite fracture mechanics, and interlaminar failure criteria which were derived empirically. To evaluate the accuracy and limits of applicability, four prepreg materials exhibiting a broad range of interlaminar fracture toughness were selected and characterized at different specimen levels as to their delamination growth behavior under various monotonic and fatigue loading conditions (mode I, mode 11 and mixed mode I/II). When comparing the mixed mode failure criteria established at the coupon level, an excellent correlation could be achieved with the experimental results obtained for higher level specimens in terms of material ranking.

1. Introduction

Compared to metallic materials, the certification of advanced composites for primary aircraft structures requires extensive experimental work which is usually represented by a test pyramid where each stage refers to a level of investigation in terms of specimen category (.Fig. 1) [1, 2]. At the lowest level of this test pyramid are “coupons” which are generic specimens (i.e., independent of application) to generate a characteristic material data base. The higher levels of the test pyramid (i.e., “laminate specimens”, “structural detail specimens”, “ subcomponents" and "full scale components”) represent non-generic specimens which are specific for a given application. They are to be defined based on engineering judgement by the aircraft manufacturer and must be approved by the certification authorities.

While analytical means to correlate stiffness related properties from lower to higher levels in the test pyramid exist, there is currently still a lack of knowledge to predict strength and life

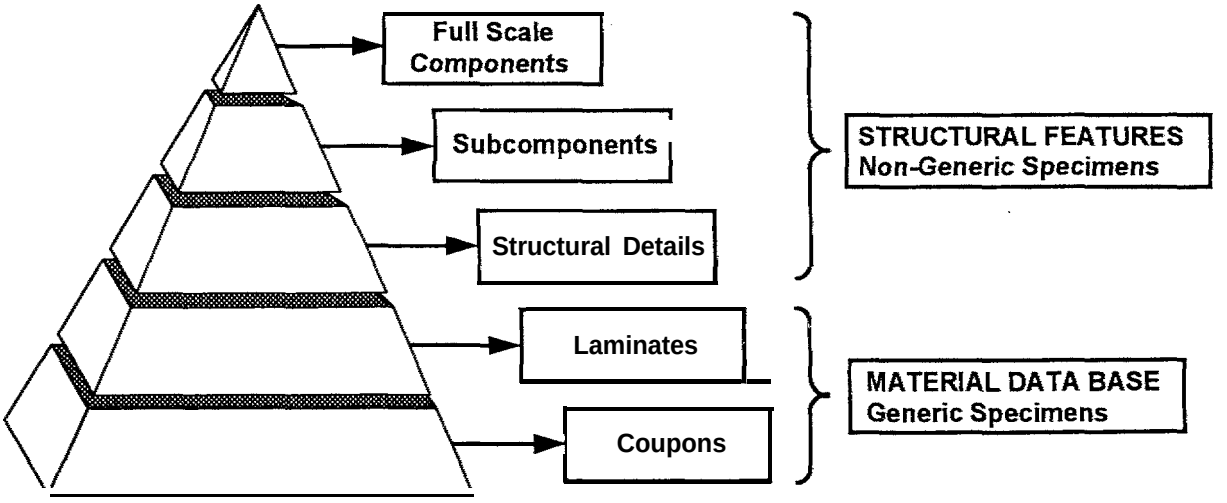

Fig. 1. Pyramid of tests for the certification of advanced composite materials for structural applications.

times of subcomponents and full scale components based on the behavior of coupon or laminate specimens. This is particularly the case when damage mechanisms such as delamination and interlaminar cracks occur, which are often regarded as the most critical modes of failure [3].

Recognizing the importance of delamination growth as major failure mechanism in advanced composite structures, a research program funded partly by the Commission of the European Communities and entitled "Damage Tolerance and Fatigue Design Methodology for Primary Composite Structures" was carried out over the past 4.5 years by CASA (Spain), BASF AG (Germany), the Fraunhofer-Institute for Strength of Structures under Operational Conditions (Germany), and the Institute of Materials Science and Testing of Plastics - University of Leoben (Austria). It was the prime objective of this program to develop and describe a procedure that bridges the gap between the various test levels and ultimately allows for a prediction (or at least an assessment) of the damage tolerance behavior of subcomponents or even full scale components based on coupon or laminate specimen properties. This could eventually lead to drastic reductions in the test program for future certifications of composite structures and thus significantly affect certification costs and times.

The purpose of this paper is to provide an overview of the work performed, and to briefly summarize the most important aspects and conclusions of this research program. More detailed information is available from the references cited throughout the paper.

2. General Approach and Methodology

The approach followed to develop a procedure to describe damage tolerance and fatigue behavior of composite structures containing delamination consisted of empirical and theoretical elements, and was divided into two major task areas. Using four different materials, task area 1 included the experimental work to empirically correlate interlaminar crack growth properties under monotonic and fatigue loading conditions at the coupon level with the corresponding performance of specimens at higher levels of the test pyramid. A further objective of this task area was to establish appropriate interlaminar failure criteria. Task area 2, on the other hand, was concerned with the development of a theoretical model and an analytical design tool to quantitatively predict residual compressive strength and fatigue life of composite components after impact based on the delamination growth criteria obtained from coupon or laminate specimens in task area 1.

2.1 Experimental Program

2.1.1 Materials and Specimen Design

To cover a broad range of material behavior in terms of interlaminar fracture toughness, the following four types of materials supplied as unidirectional prepregs were included in the experimental program:

Material 1:	Rigidite® 5239-1/G30-500	(brittle epoxy matrix)
Material 2:	Rigidite® 5259/G30-500	(toughened epoxy matrix)
Material 3:	Rigidite® 5276/G30-500	(modified toughened epoxy matrix)
Material 4:	APC-2/AS4®	(thermoplastic polyether ether ketone matrix)

While Materials 1 to 3 (supplier: BASF AG) consisted of different 180 "C-curable epoxy resin systems but of the same carbon fiber type (Celion® G30-500112 K) and were produced to prepregs of the same nominal fiber areal weight ($135 \pm 5\,g/m^2$) and resin content (35 ± 3 %), prepregs of Material 4 (supplier: ICI) contained a different fiber type (Hercules AS4) with a slightly higher fiber areal weight ($\mathbf{14.5} \pm \mathbf{5}\ g/m^2$) and lower resin content (29 ± 3 'A). However, both fiber types used are similar in their strength and stiffness properties, and all specimens were manufactured to a fiber volume content of 58 ± 5 ·/₀, thus allowing for a direct comparison of the effect of matrix toughness on damage tolerance test results.

Included in the experimental program were tests at four specimen levels. While only unidirectional specimens were used at the coupon level, multidirectional specimens, depicted in Fig. 2 accentuating the interrelated specimen design, with ply orientations of 0°, 90°, +45° and -45° were chosen for the tests at higher levels.

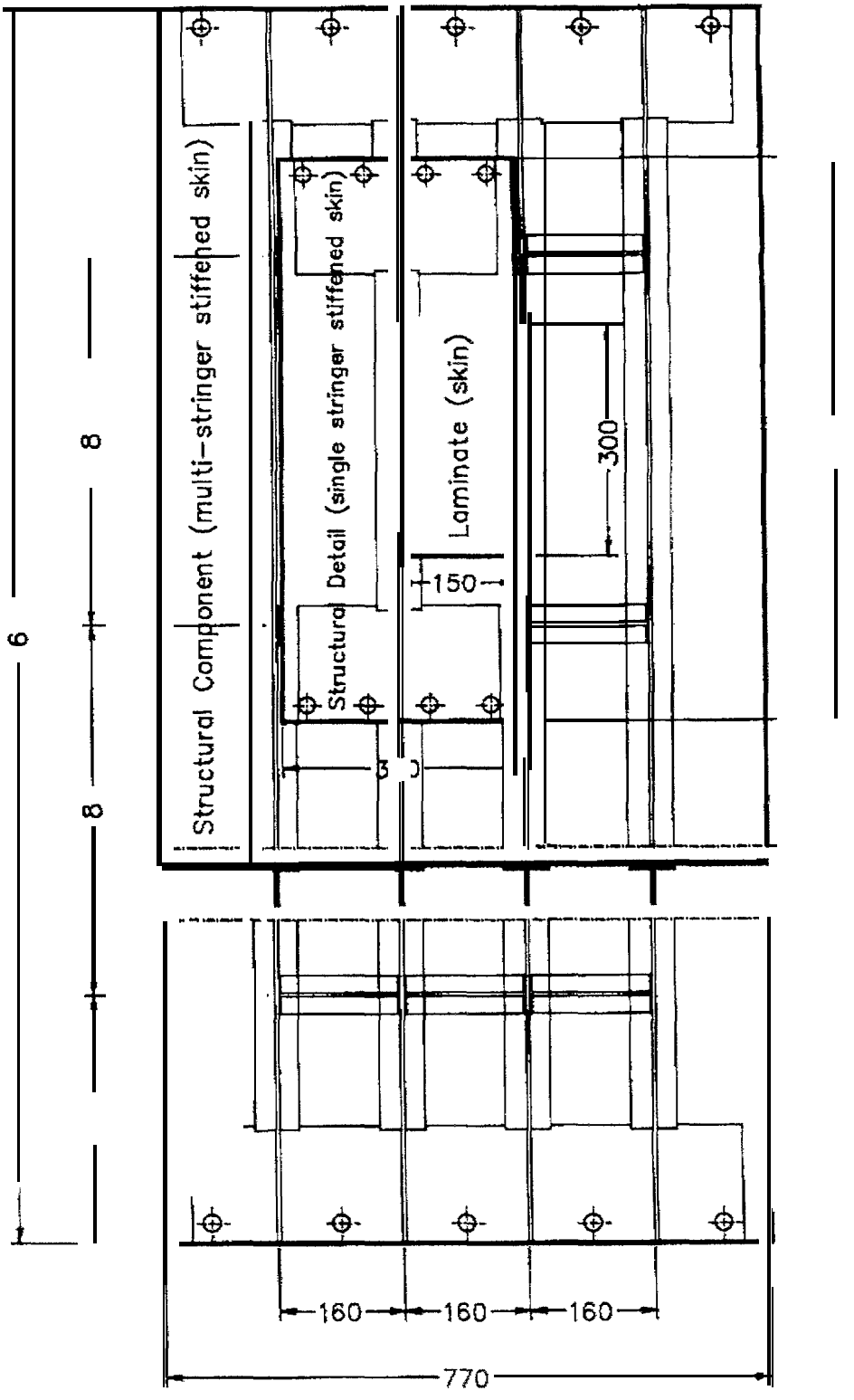

Fig. 2. Interrelated specimen design of laminate specimens, structural detail specimens and subcomponents (dimensions in mm).

Further information as to the materials, their basic mechanical properties, the specimen design and processing conditions is described elsewhere [4 - 6].

2.1.2 Damage Tolerance Testing

The damage tolerance tests conducted at the various specimen levels under monotonic and fatigue loading conditions to deduce the required failure criteria and to empirically assess the translation of coupon properties into laminate properties and into the performance of structural detail specimens and subcomponents, are listed in Tables 1 and 2, respectively. Also included in these tables is information on the types of tests performed and the materials tested along with the impact energies applied to certain specimens prior to monotonic or fatigue testing.

The monotonic damage tolerance (MDT) tests (see Table 1) included experiments at four specimen levels. At the coupon level double cantilever" beam (DCB) tests, end notched flexure (ENF) and mixed mode bending (MMB) tests were performed with all four materials to determine the critical strain energy release rates under mode I (G_{Ic}), mode II (G_{IIc}) and mixed mode ($G_{I/IIc}$) loading conditions, respectively.

At the laminate level the monotonic tests included compressive strength measurements of undamaged specimens and residual compressive strength measurements of impact-damaged specimens (i.e., compression after impact (CAI) tests) for all four materials. As to the specimens damaged by impact prior to the compressive test, two test series were carried out. In one series the impact energy was kept constant for all materials at 35 J, in the other series specimens of each material were impacted to an energy level which resulted in the development of a so-called "barely visible impact damage". The latter energy levels are listed in parenthesis in Table 1.

Analogous to the laminate specimen level, compressive tests using undamaged and impact-damaged specimens were performed at the structural detail and subcomponent levels. However, to contain the test program within certain limits, the number of materials investigated at these levels was reduced to 3 and 2, respectively.

For a similar reason the fatigue damage tolerance (FDT) tests had to be contained to three levels of investigation, thus omitting the costly and time consuming tests at the subcomponent level (see Table 2). Here too, DCB, ENF and MMB tests have been performed with all materials to characterize the delamination growth behavior under cyclic loads in terms of crack growth rates, da/dN (a being the crack length, and N the number of loading cycles), versus the cyclic strain energy release rate range, ΔG, for the various loading modes again indicated by the subscripts I for mode I, II for mode H, and I/II for mixed

Table L Monotonic damage tolerance **(MDT)** tests at the various levels of the test pyramid.

Specimen Level	Type of Test	Materials	Impact Energy
Coupon Specimens	DCB Test: G_{Ic} ENF Test: G_{IIc} MMB Test $G_{I/IIc}$	Materials 1 to 4	--
Laminate Specimens	Compressive Strength	Materials 1 to 4	--
	CAI-Strength	Material 1	35 J (35 J)
		Material 2	35 J (50 J)
		Material 3	35 J (45 J)
		Material 4	35 J (42 J)
Structural Detail Specimens	Compressive Strength	Materials 1 to 3	
	CAI-Strength	Materials 1 to 3	45 J
Subcomponent Specimens	Compressive Strength	Materials 2 and 3	--
	CAI-Strength	Material 2 Material 3	70 J

Table 2. Fatigue damage tolerance (FDT) tests at the various levels of the test pyramid.

Specimen Level	Type of Test		Materials	Impact Energy
Coupon Specimens	DCB Test: da/dN vs. ΔG_I ENF Test: da/dN vs. ΔG_{II} MMB Test: da/dN vs. $\Delta G_{I/II}$		Materials 1 to 4	--
Laminate Specimens	FAI Tests:	S_{max}-N_f Behavior	Materials 1 to 4	35 J
		$(dA/dN)_{app}$ vs. $\Delta G_{t,app}$	Material 4	35 J
	FAD Tests: $(dA/dN)_{app}$ vs. $\Delta G_{t,app}$		Materials 1 to 4	artificial circular delamination (diameter =60 mm) between plies 5 and 6
Structural Detail Specimens	FAI Tests:	S_{max}-N_f Behavior	Materials 1 to 3	45 J
		$(dA/dN)_{app}$ vs. $\Delta G_{t,app}$	Materials 1 to 3	45 J

mode I/II loading conditions. The value of ΔG is defined as the difference between the maximum and the minimum G-values, G_{max}-G_{min}, associated with the maximum and minimum loads in a fatigue cycle. The tests were carried out under load control with sinusoidal loads at a frequency of 5 Hz and an R-ratio (minimum-to-maximum load ratio in a cycle) of 0.1.

As was the case for monotonic tests, two series of investigation were performed to characterize the fatigue damage tolerance of all 4 materials at the laminate level. Again, in one test series, designated fatigue after impact (FM) tests, the impact level prior to fatigue testing was kept constant at 35 J for all materials. Subsequently fatigue tests were performed under sinusoidal compressive loads at a frequency of 3 Hz and an R-ratio of 10 (note that this R-ratio for compressive loads corresponds to the value of 0.1 at the coupon level under tensile or bending loads). The tests were conducted with constant load amplitude at various load levels and the following parameters were monitored:

specimen life time in terms of number of cycles to failure, N_f, for each maximum compressive stress level, S_{max} (i.e., S_{max}-N_f behavior),

specimen compliance as a function of loading cycles (continuous recording),

- projected delamination area, A, by an ultrasonic C-scan technique at certain numbers of loading cycles, N, prior to ultimate failure.

From the number of fatigue cycles, the projected delamination area and the corresponding specimen compliance, apparent delamination growth rates per cycle, $(dA/dN)_{app}$, and total apparent cyclic strain energy release rates, $\Delta G_{t\,app}$, have been deduced, thus allowing to characterize a material in terms of its delamination growth behavior similar to the description of the kinetics of cyclic crack growth at the coupon specimen level. The expression "apparent" indicates, that the raw data of the projected delamination area have been used in these calculations, without accounting for the fact that the total true fracture surface area is probably much larger, due to overlaps of delamination in different plies and as a result of transverse cracks. Further details as to this test procedure and the data reduction scheme are described elsewhere [5].

Since the laminate specimens, when impacted with constant energy, developed different delamination areas and damage patterns depending on the material [7, 8], in the second series of fatigue tests at the laminate level, laminates with artificial circular delaminations (see Table 2) of constant size were investigated (fatigue with artificial delamination (FAD) tests) to support the theoretical modelling efforts. Equivalent to the test conditions and

the procedure outlined above, delamination growth kinetics was characterized as $(dA/dN)_{app}$ vs. $\Delta G_{t\,app}$.

At the detail specimen level only Materials 1, 2 and 3 were investigated and the fatigue life, N_f, of impacted specimens (impact energy of 45 J) was recorded for various maximum cyclic stress levels S_{max}. Other test conditions (i.e., waveform, frequency and R-ratio) were identical to those at the laminate specimen level. Also analogous to the laminate specimen level, delamination growth kinetics was characterized as $(dA/dN)_{app}$ vs. $\Delta G_{t,app}$.

2.2 Basic Assumptions and Elements of the Theoretical Model

The theoretical basis for the new analytical design tool, a schematic presentation of which is shown in Fig. 3, includes laminate plate theory, stability theory, composite fracture mechanics, and failure criteria which were derived empirically within this project. In general, two basic forms of buckling, illustrated in Fig. 4 and designated sublaminate buckling (e.g., revealed also by specimens containing single artificial delaminations) and global buckling (i.e., ordinary skin buckling as it occurs in areas damaged by impact), maybe discerned.

The model idealizes a laminate plate with delamination by a system of parallel and in-series springs. A key issue of the model is that a buckling sublaminate does not carry more than its buckling load even when the total external load is still rising. The buckling loads calculated by a Rayleigh-Ritz method depend on the size of the individual sublaminate and change the slope of the overall load deformation curve (see Parts I and II in Fig. 3).

Based on load-deformation curves for consecutive damage states in a fatigue loading situation, total cyclic strain energy release rate ranges, ΔG_t, are calculated via a compliance technique. In combination with a proper failure criterion (i.e., $dA/dN = f(\Delta G_t)$) damage growth rates and residual fatigue life may be calculated (see Part III in Fig. 3).

For sublaminate buckling the G-value distribution along the delamination front was derived by finite element analysis [9]. Geometry, boundary and loading conditions of the finite element model were that of a laminate specimen with an artificial circular delamination. More details as to the theoretical model are described explicitly in [4, 10].

3. Results and Discussion

3.1 General Remarks and Analytical Findings

When comparing the experimental findings and results of coupon specimens with those of laminate, structural detail and subcomponent specimens, several things should be kept in

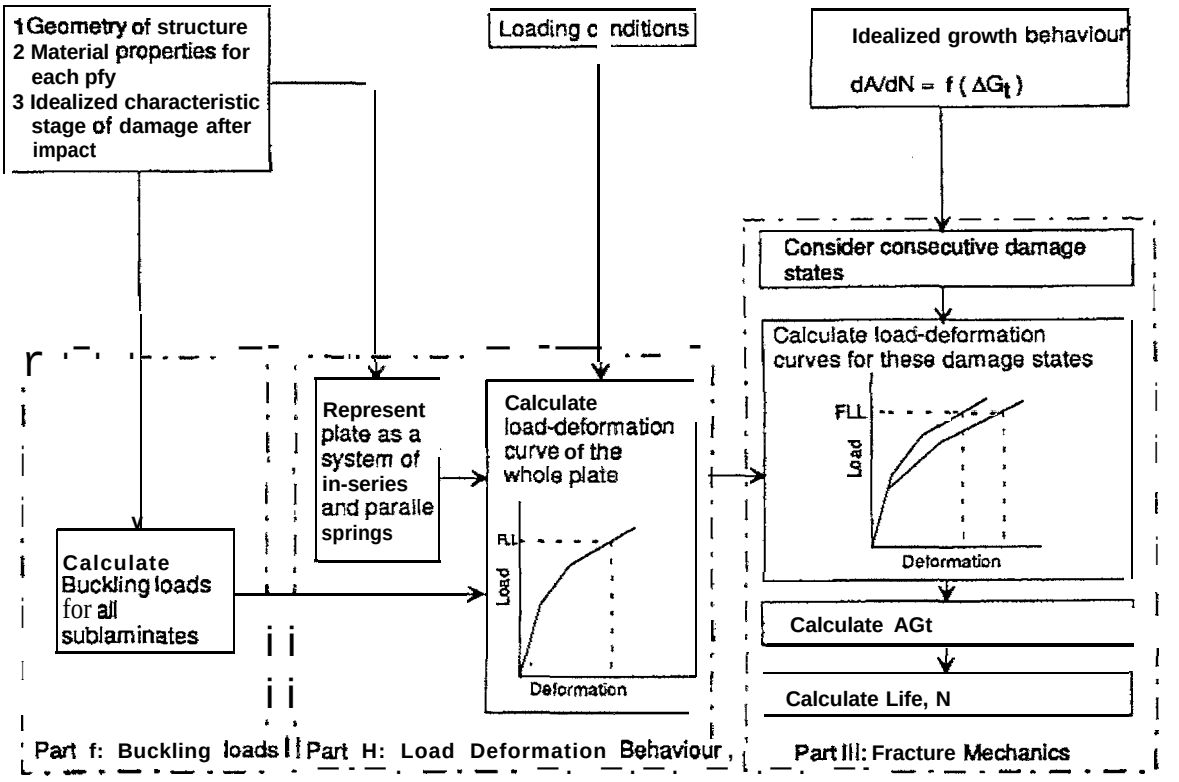

Fig. 3. Schematic representation of the theoretical model to predict damage growth (FLL...fatigue load level).

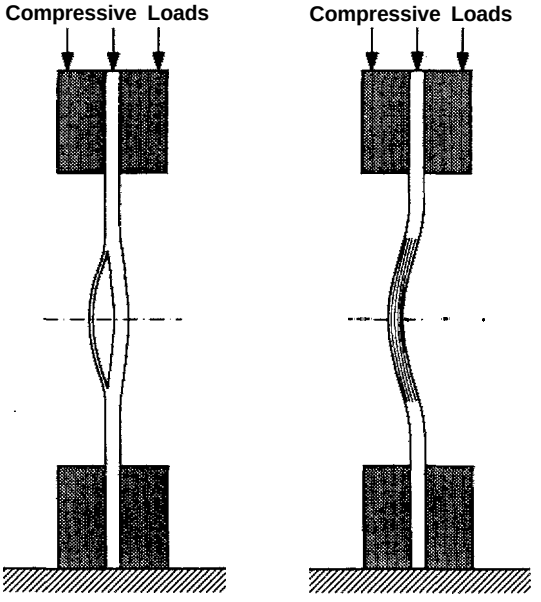

Fig. 4. Forms of buckling in laminates under compression; (a) laminate with a single (artificial) delamination; (b) laminate with delaminations generated by impact.

mind. First, while the higher level specimens consisted of multidirectional ply orientations, unidirectional specimens have been used at the coupon level (i.e., DCB-, ENF- and MMB-specimens) to generate interlaminar failure criteria. Second, in contrast to the single delaminations which have been characterized at the coupon level, specimens at higher levels of the test pyramid exhibited complex darnage patterns upon impact, consisting of delaminations at various interply regions, transverse cracks and shear cracks, and also of a multitude of broken fibers [7, 8].

Furthermore, while tests at the coupon level were limited to mode I, mode II and various mixed mode I/II loading conditions, in a strict sense delamination in higher order specimens under compressive loads also experience a mode III component. However, the results of the finite element calculations shown in Fig. 5 reveal, that at least for single circular and elliptical delaminations causing sublaminate budding (see Fig. 4a), the crack driving forces at the delamination front are dominated by mode I, mode II or mixed mode I/II conditions, thus justifying that the experimental work was also restrained to the loading modes I and H and combinations thereof. More specifically, for sublaminate buckling the theoretical calculations have shown the following critical mode conditions (CMC) for positions where the total strain energy release rate, $G_t = G_I + G_{II} + G_{III}$, reveals a maximum:

Critical mode condition for circular delaminations: $(G_I/G_{II})_{CMC} \approx 2/1$
Critical mode condition for elliptical delamination: $(G_I/G_{II})_{CMC} \approx 5/1$

The fact, that Fig. 5a for circular delaminations also reveals that under compression the maximum G_t-values in the laminate plane exist at the delamination boundaries perpendicular to the loading axis ($G_t = G_I + G_{II}$ at this position), implies that a circular delamination should grow faster at these locations and develop from a circular into an elliptical shape. This conclusion from analytical considerations was found to be in good agreement with experimental findings of this project. In other words, the relevant critical mode conditions for sublaminate buckling, as it occurs for example in specimens containing artificial defects, range from mode I-to-mode H ratios of 2/1 to 5/1.

Although no detailed calculations have been performed for global buckling of laminates as it is usually observed with impacted specimens which are subsequently loaded in compression (Fig. 4b), based on the appearance of this deformation phenomenon it is assumed that the critical mode condition in this case is dominated by mode H.

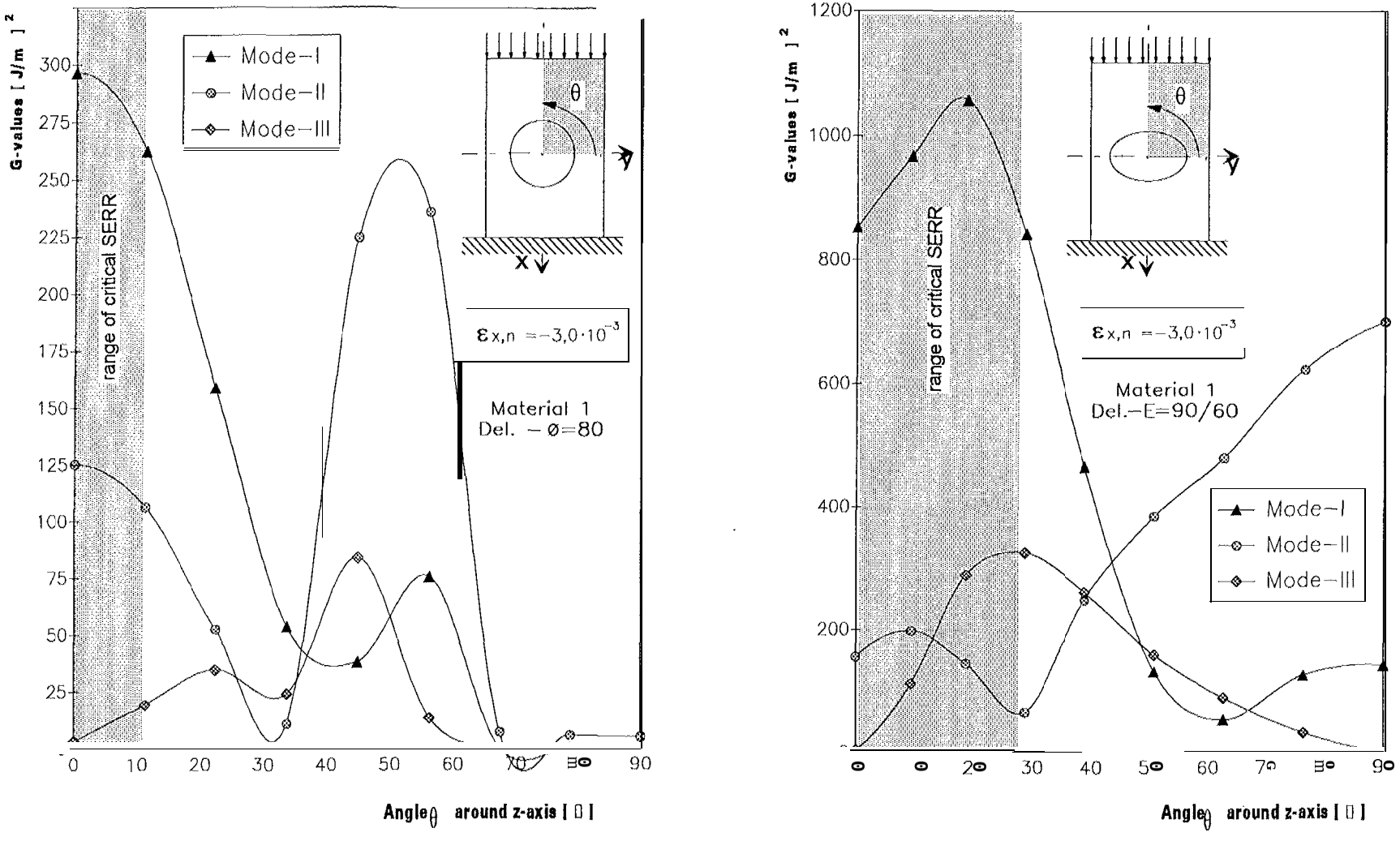

Fig. 5. Calculated strain energy release rate range (SERR) distribution along the delamination front for sublaminate buckling in Material 1 at a nominal compressive strain, $\varepsilon_{x,n}$ = 0,3 %; (a) circular delamination (diameter: 80 mm); (b) elliptical delamination (main axis dimensions: 90 mm and 60 mm) [9].

3.2 Empirical Correlation of Test Results

As stated above, a principal objective of this study was to correlate the interlaminar crack growth resistance at the coupon level with the damage tolerance behavior of specimens at higher levels of the test pyramid. Thus, the resistance to delamination growth in coupon specimens is depicted in Fig. 6 and Fig. 7, where the interlaminar crack growth envelopes of the four materials are compared for monotonic loading and fatigue loading (stable crack growth range, $da/dN = 10^{-4}$ mm/cycle), respectively. Also indicated in the diagrams is the CMC range for sublaminate buckling for mixed mode L/mode D-ratios from 2/1 to 5/1. The failure envelopes represent calculated curves and were obtained from experimental results through a least square curve fitting procedure [6,11]. For the case of fatigue loading, similar failure envelopes were generated for the fatigue threshold region ($da/dN = 10^{-8}$ mm/cycle) and the fast crack growth regime (da/dN = 10-1mmlcycle)[11, 12].

While the failure envelopes for monotonic and fatigue loading reveal distinctly different shapes, the following material ranking may be established in interlaminar crack growth resistance at the coupon level, independent of loading conditions:

Material 4 > Material 3 > Material 2 > Material 1

The same qualitative correlation in terms of material ranking was found for the damage tolerance behavior of laminate specimens and structural detail specimens, based on the absolute numbers in CAI-strength (Fig. 8) and FAI-strength (defined as the maximum cyclic stress level after impact that can be sustained for 10^6 loading cycles; Fig. 9).

Due to the predominance of the mode II loading condition experienced by laminates during the impact and during the subsequent application of compressive loads, values for G_{IIc} obtained from coupon tests might be most relevant for a quantitative correlation of the CAI performance at higher specimen levels. Therefore the absolute results of the CAI experiments of the higher order specimens are plotted in Fig. 10 over the corresponding G_{IIc}-values determined experimentally for each material. It is apparent from this figure, that the improvement in G_{IIc} from Material 1 to Material 4 by a factor of 4.3 leads to a corresponding improvement of CAI strength at higher specimen levels of only about 1.5. In other words, toughness improvements achieved at the coupon level do not filly translate into subcomponent behavior, the degree of performance translation being only approximately 35 % for monotonic loading conditions.

Similarly, the results of the FAI tests at the laminate and structural detail level are plotted over the corresponding ΔG_{II}-values of the various materials in the stable crack growth region in Fig. 11. As with the MDT tests, a good correlation is found. However, in contrast

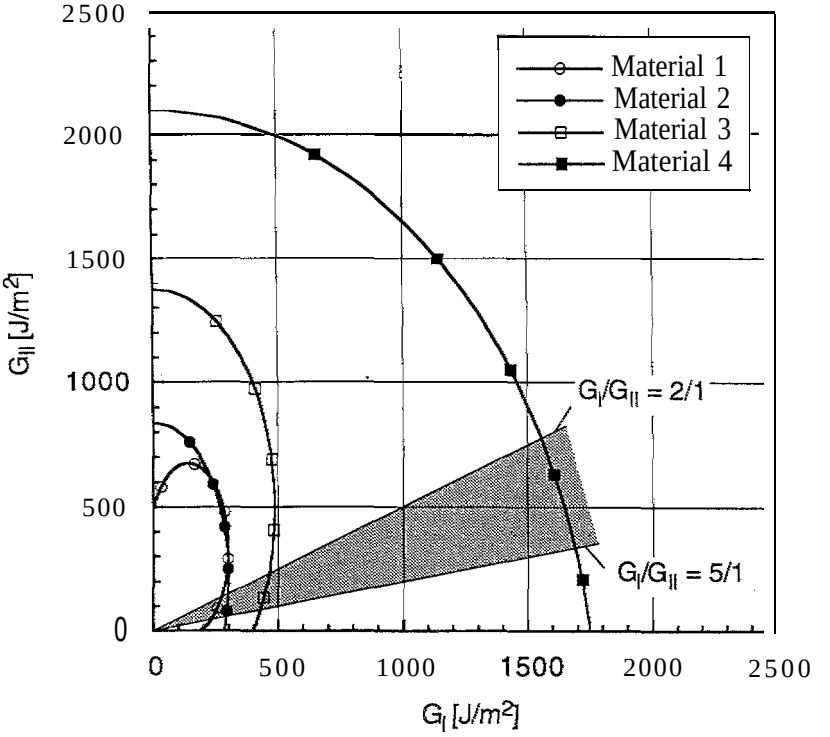

Fig. 6. Interlaminar failure envelopes derived from coupon tests under monotonic loading conditions (failure envelopes from ref. [11]).

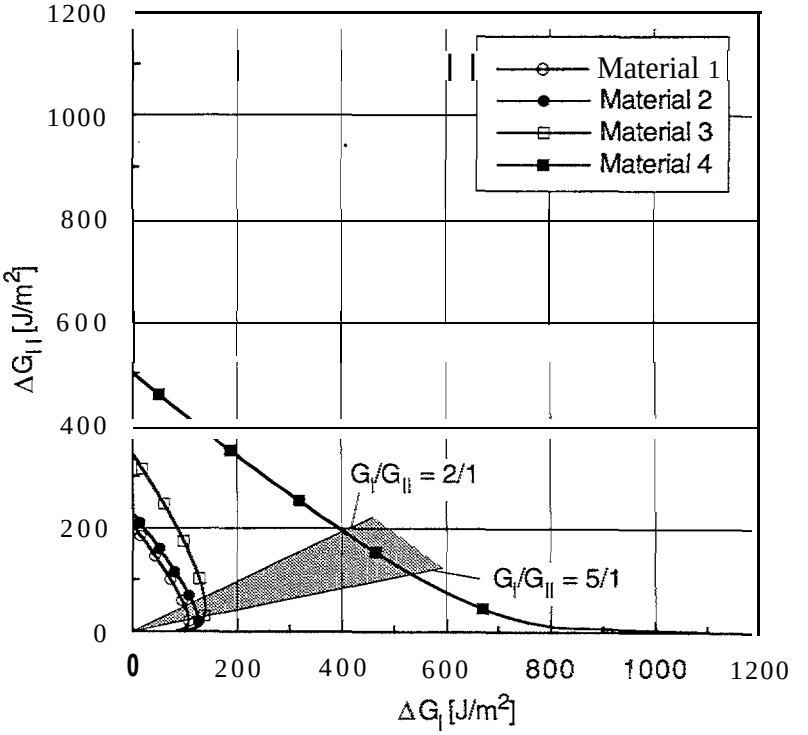

Fig. 7. Fatigue Delamination growth envelopes (stable delamination growth rate; $da/dN = 10^{-4}$ mm/cycle) derived from coupon tests (failure envelopes from ref. [11]).

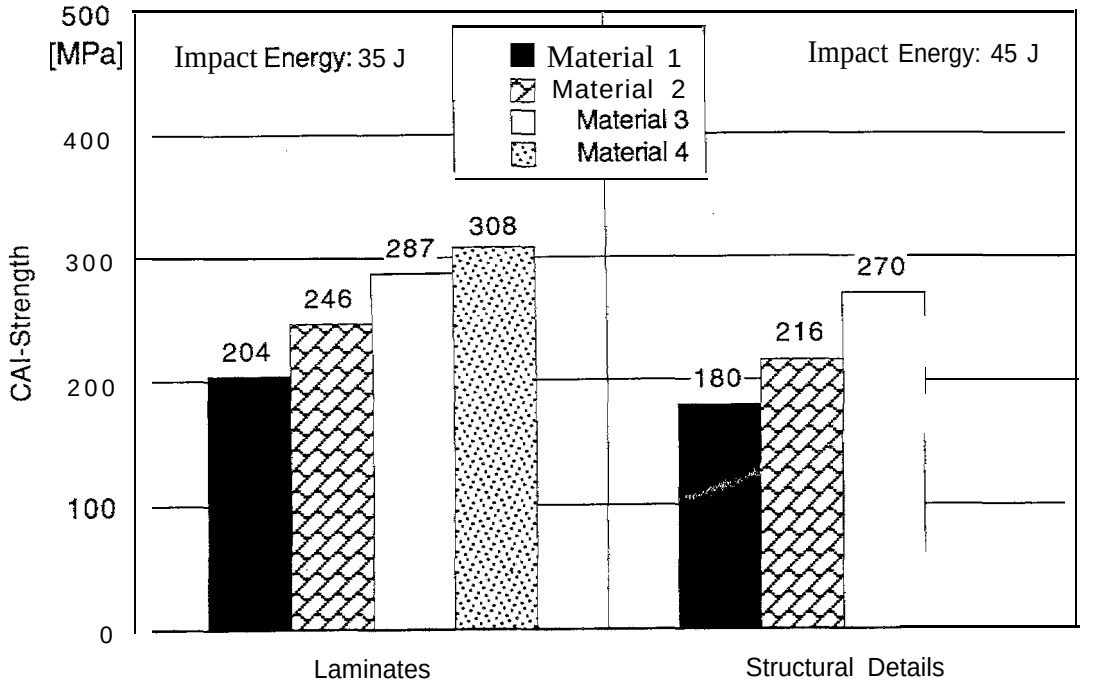

Fig. 8. Monotonic damage tolerance of laminate specimens and structural detail specimens.

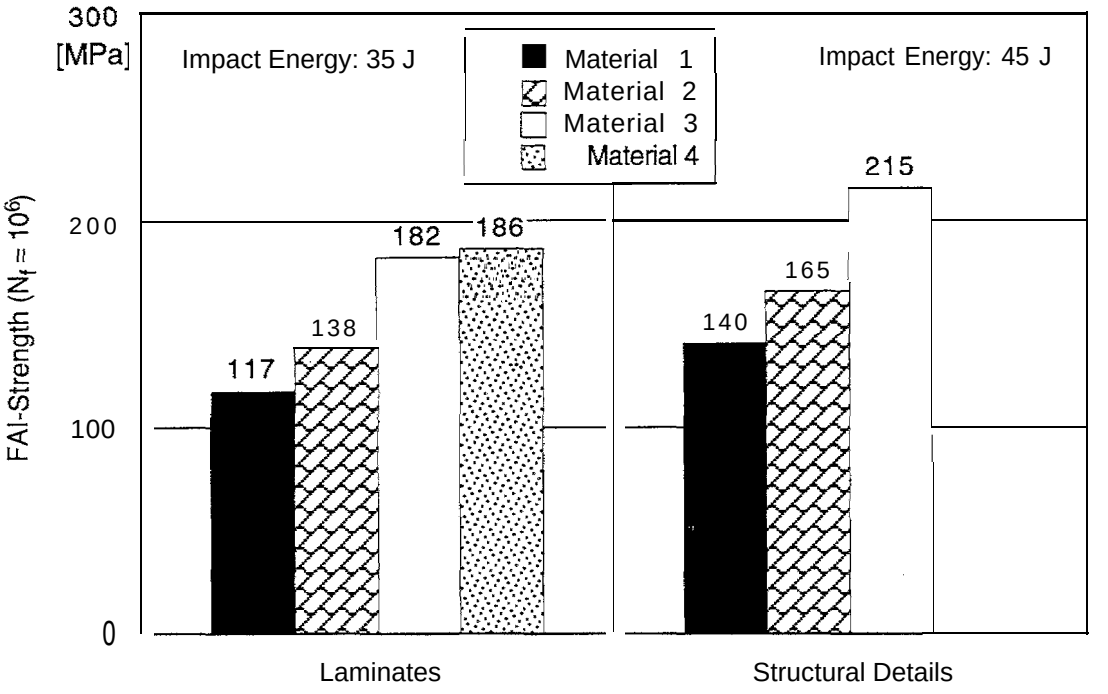

Fig. 9. Fatigue damage tolerance of laminate specimens and structural detail specimens.

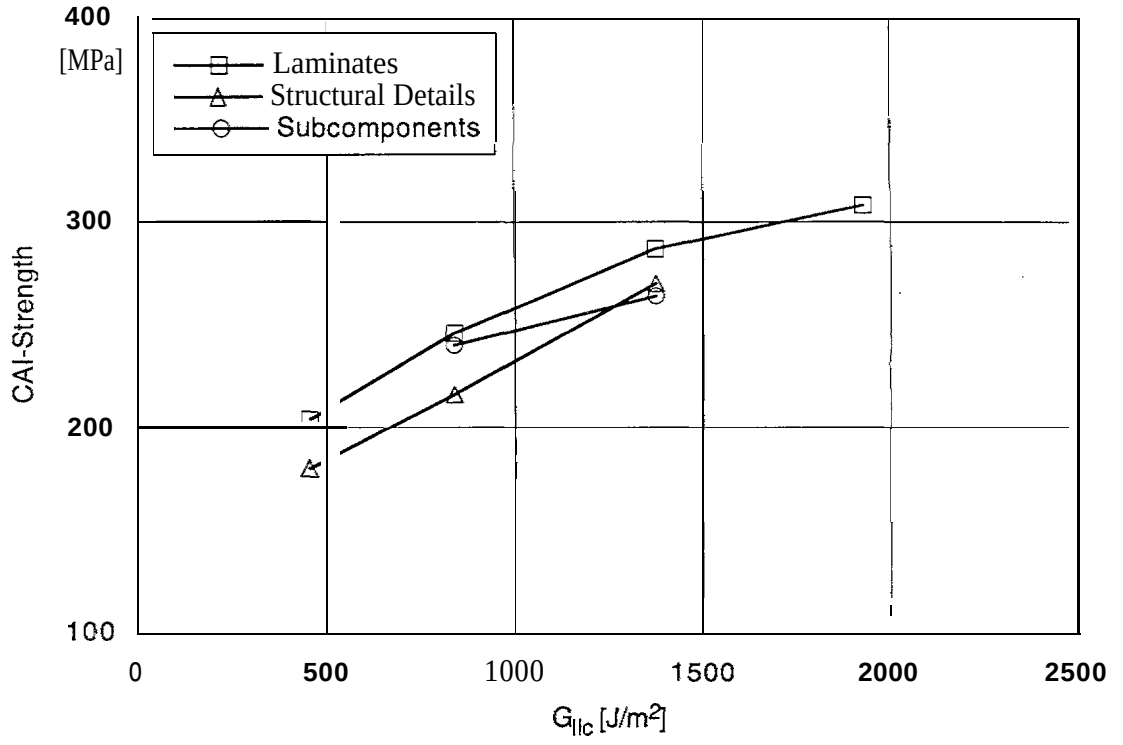

Fig. 10. Compression after impact (CAI) strength for various specimen levels as a function of mode II interlaminar fracture toughness, G_{IIc}, of coupon specimens.

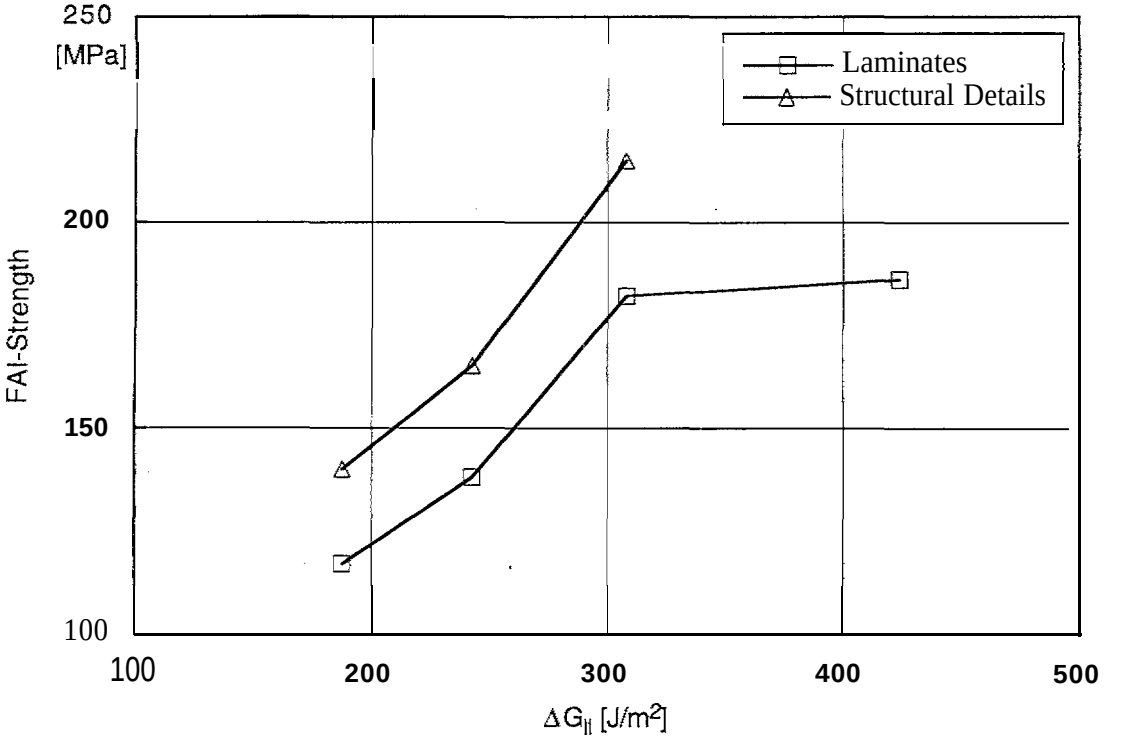

Fig. 11. Fatigue after impact (FAI) strength ($N_f = 10^6$ cycles) as a function of ΔG_{II} ($da/dN = 10^{-4}$ mm/cycle) of coupon specimens.

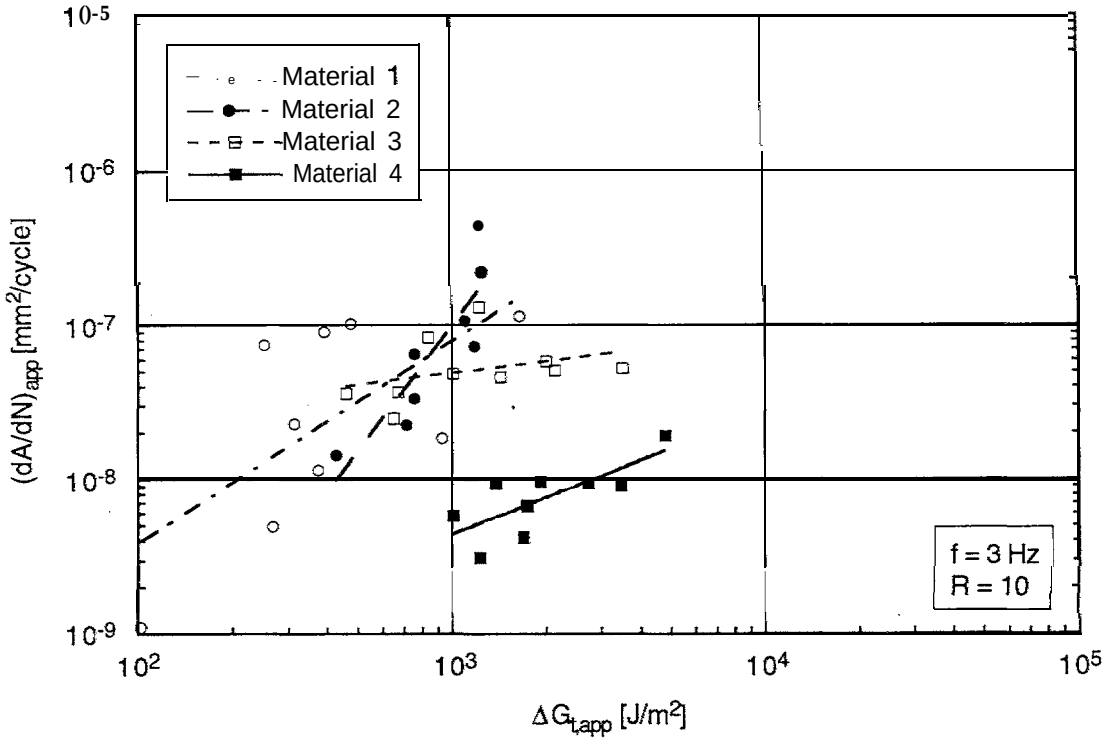

Fig. 12. Apparent delamination growth behavior of laminate specimens with artificial delamination under repeated sublaminate buckling.

to the MDT tests, a performance translation of approximately 70 % was found in the FAI tests for the range of materials investigated.

3.2 Prediction Model

For current composite structures, operational loading is not allowed to exceed skin buckling loads. Therefore the prediction model considers sublaminate buckling, which occurs at loads significantly lower than those for skin buckling but remains active with increasing compressive loads up to total failure. A budding form close to sublaminate buckling is assumed when delamination are in the vicinity of supporting stiffeners and loads are far above skin buckling.

As pointed out before, fatigue delamination growth experiments with laminates containing artificial delaminations (FAD tests) and revealing sublaminate buckling have been performed to test the prediction model. These results of the fatigue delamination growth tests are shown in Fig. 12. Not surprisingly, considering the details of this test technique, the scatter of the data is substantial. Also, the absolute numbers in the $\Delta G_{t,app}$-values reduced from these experiments differ significantly from those found for the various delamination growth regimes of these materials at the coupon level (see Fig. 7 for comparison). And yet, despite all these shortcomings it appears that the relative ranking of materials qualitatively

corresponds rather well again to the ranking of materials in fatigue delamination growth resistance at the coupon level.

Subsequently, a refined method was developed to adjust the apparent damage growth data from projected damage areas to also account for compliance changes associated with the generation of additional fracture surfaces (e. g., transverse cracks, etc.). Applying this refinement method to the raw data of laminate specimens with artificial circular delamination yielded the so-called "equivalent" delamination growth results ($(dA/dN)_{equ}$ vs. $\Delta G_{t,equ}$) depicted in Fig. 13. Thus, a reasonable quantitative correlation is observed when comparing the total strain energy release rate ranges, ΔG_t, over which delamination growth was observed for the various materials at the coupon level, to the corresponding $\Delta G_{t,equ}$-values obtained from laminate specimens with artificial delamination. The lower bound values of the coupon specimens in Fig, 13 were deduced from the fatigue failure envelopes of the threshold regime for a mixed mode ratio $G_I/G_{II} = 2$ (reflecting the critical situation of the original circular delamination); the upper bound values for coupon specimens were taken from monotonic interlaminar failure envelopes (compare Fig. 6) for $G_I/G_{II} = 5$, the critical mode condition for elliptical delamination.

Finally, delamination growth areas calculated on the basis of equivalent crack growth data were found to be in good agreement with experimental findings, as is shown in Fig. 14, The computer program developed for this procedure is called "IMPACT" and is ready for use. The program is written in FORTRAN and runs also on 386 PC%. The software is available on a discette and is well documented. A more detailed description of the prediction model is provided in [4, 10, 13].

4. Summary and Conclusions

The main purpose of this project was to investigate delamination growth behavior in advanced composites at various specimen levels of the test pyramid under both monotonic and fatigue loading conditions. An extensive experimental program was carried out including four different carbon fiber composite systems with polymer matrices of different toughness. While the monotonic damage tolerance tests included experiments at four specimen levels (coupon specimens, laminate specimens, structural detail specimens and sub components), fatigue damage tolerance was investigated at three specimen levels only (leaving out subcomponent tests).

For several of the tests performed, the test methodologies as well as the data reduction schemes were developed within the framework of this project. Also of importance for the data analysis were theoretical calculations for composite laminates containing artificial

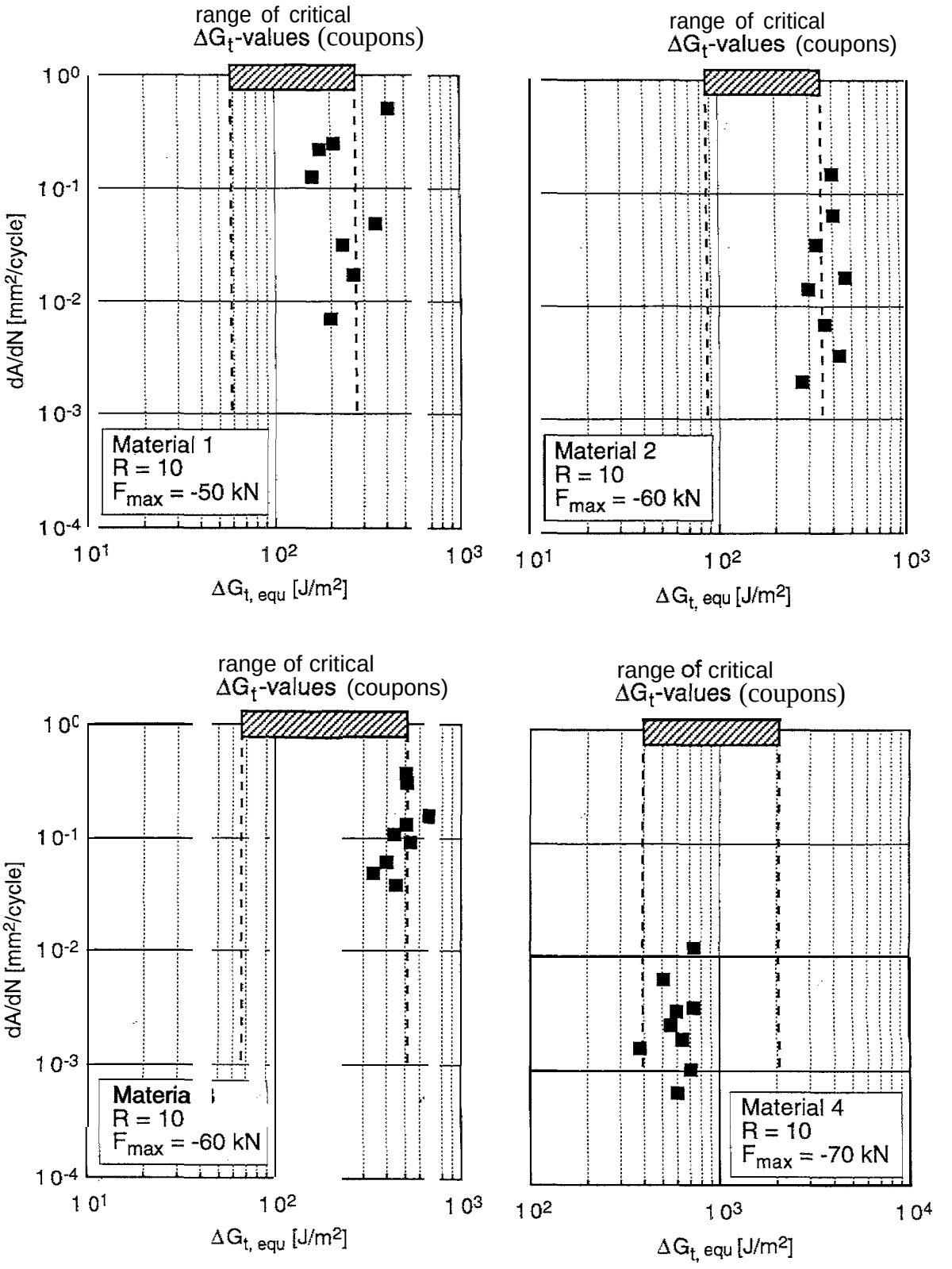

Fig. 13. Equivalent delamination growth behavior of laminate specimens with initial artificial delaminations under repeated sublaminate buckling; also indicated for comparison are the ranges of AG_t obtained from coupon specimens.

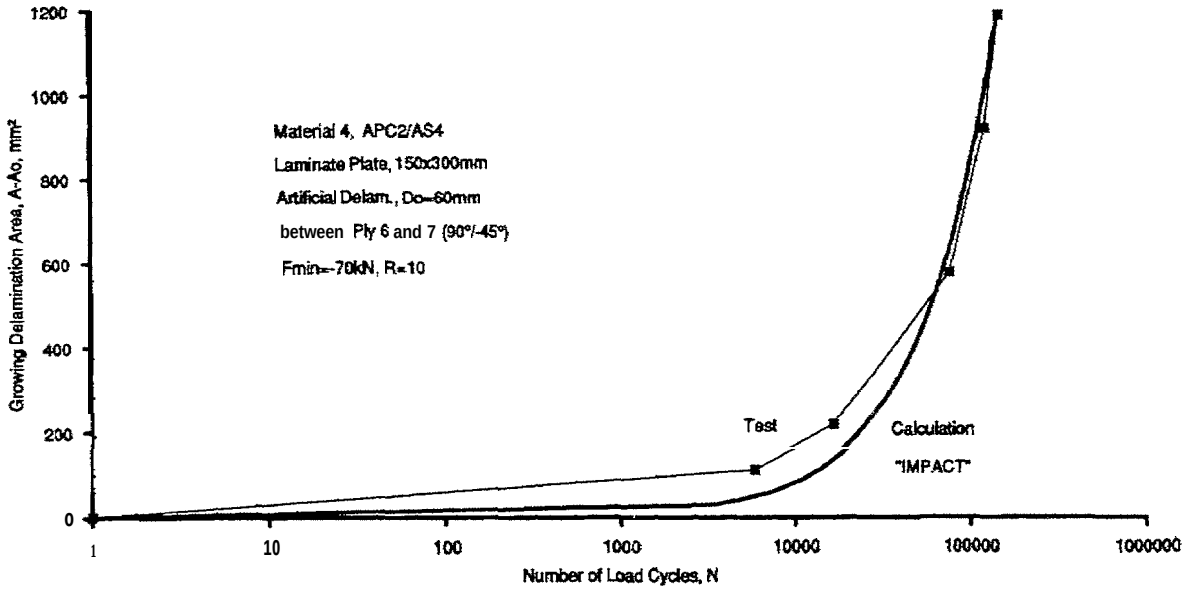

Fig. 14. Comparison of measured and calculated delamination growth data for Material 4 containing a single artificial delamination.

delamination, describing the distribution of strain energy release rates at the delamination boundaries and providing the information on critical mode conditions.

In conclusion, it could be shown that reasonable to excellent qualitative and quantitative correlations exist in terms of ranking the materials as to their damage tolerance behavior under monotonic (compression after impact, CAI) and fatigue (fatigue after impact, FAI) loading conditions. While the performance translation from the coupon level to higher order specimens was found to be only 35 % for CAI behavior, a value of approximately 70% was found in the FAI tests for the range of materials investigated.

In addition, a new analytical design tool, which includes laminate plate theory, stability theory, composite fracture mechanics, and interlaminar failure criteria which were derived empirically within this project, was developed. Reasonable predictions can be expected for sublaminates at load levels below skin buckling and for sublaminates close to supporting stiffeners at load levels above skin buckling. However, further research is needed to model the impact damage and global buckling more accurately.

Acknowledgments

The research program summarized in this paper was supported by the European Community under BRITE/EURAM Contract No. BREU.0182.C (Project No. BE-3038-89). The authors would like to express their gratitude to M. Cvitkovich (University of Leoben), M. Huertas (CASA), T.d. Jonge (FhG-LBF), J. Sánchez Gómez (CASA) and A. Schöpfel (FhG-LBF) for their valuable contributions to this program. The technical assistance of Mr. von den Driesch of the Commission of the EC is also gratefully acknowledged,

References

[1] R.W. Lang, G. Herrmann and K. Schneider, in "Advanced Materials: The Challenge for the next Decade", G. Janicki, V. Bailey and H. Schjelderup (eds.), Proc. of the 35th Intern. SAMPE Symposium 1990, U.S. Chapter, Anaheim, April 1990, p. 2245 -2259.

[2] K. Schneider and R.W. Lang, in "Plastics-Metals-Ceramics", H.L. Hornfeld (cd.), Proc. of the 11th Int. SAMPE Conference 1990, European Chapter, Basel, May 1990, p. 381-394.

[3] A.G. Miller, D.T. Lovell and J.C. Seferis, Composite Structures 27 (1994), p. 193 - 206.

[4] Final Technical Report to the BRITE/EURAM Commission of the European Community (contract no. BREU-0182C), March 1995.

[5] J.J. Gerharz, A. Schöpfel, M. Cvitkovich, H. Huth and R. W. Lang, Proceedings of the 17th ICAF-Symposium, Stockholm 1993, A.F. Blom (cd.), Vol. 1, p. 733.

[6] M. Cvitkovich and R.W. Lang, Proceedings of the European Conference on Composite Materials ECCM-CTS2, Hamburg, Germany, Sept. 13-15, 1994, p. 149 -157.

[7] M. Sobota, Study Project, Institute of Materials Science and Testing of Plastics, University of Leoben, Austria (1993).

[8] R. Rittenbacher, Study Project, Institute of Materials Science and Testing of Plastics, University of Leoben, Austria (1995).

[9] A. Schöpfel and J.J. Gerharz, "Determination of Active Modes in Impact Damaged Laminates under Compression", LBF-Bericht Nr. 7095, Feb. 15, 1993.

[10] T.d. Jonge and J.J. Gerharz, "Prediction Method of Residual Strength and Fatigue Life for Delaminated Composite Structure", LBF-Bericht Nr. 7096, April 26, 1993.

[11] M. Cvitkovich, Doctoral Dissertation, Institut of Materials Science and Testing of Plastics, University of Leoben (in preparation).

[12] R.W. Lang, M. Cvitkovich, J.J. Gerharz, A. Lavia and M. Heym in "High Tech in Salzburg - Creativity in Advanced Materials and Process Engineering" R.W. Lang (cd.), Proc. of the 16th Int. SAMPE Conference 1995, European Chapter, Salzburg, May 30- June 1, 1995 (to be published).

[13] J.J. Gerharz et.al., in "High Tech in Salzburg - Creativity in Advanced Materials and Process Engineering" R.W. Lang (cd.), Proc. of the 16th Int. SAMPE Conference 1995, European Chapter, Salzburg, May 30 - June 1, 1995 (to be published).